Magnetotelluric Data Acquisition in a High-Noise Environment: Results from the Steamboat Hills Geothermal Complex, Nevada, USA

Daniel Feucht, Christopher Gates, Robert Selwood, Madeline Churchill, and Robin Zuza

Ormat Technologies, Inc., 6140 Plumas St, Reno, NV 89519

Keywords

Geophysics, magnetotellurics, Ormat, Steamboat, geothermal exploration, MeB analysis

ABSTRACT

Magnetotelluric (MT) geophysical surveys can inform drilling and resource management decisions throughout the development lifetime of a geothermal field. However, operators of developed fields that lack legacy MT data may be reluctant to collect new or in-fill data due to concerns that electromagnetic noise generated by the power plant will result in poor data quality. Modern advances in magnetotelluric instrumentation, field practices, and data analysis have made it possible to collect high quality MT data in these high noise environments. A broadband MT survey designed to test these capabilities was recently collected over the Steamboat geothermal system in Reno, Nevada, USA. The Steamboat geothermal complex, which currently generates a combined 79 MW from six geothermal power plants spread over ~4 km^2, provides both a high noise environment and a well characterized geothermal reservoir in which to test this assertion.

Analysis of magnetotelluric time series and transfer functions demonstrates that reasonably high-quality MT data can be achieved within <500 m of power plant infrastructure. Field practices that influenced data quality include careful survey design, long duration recording times (>40 hours), and use of a dedicated remote reference. Three-dimensional (3D) inversion of the resulting MT data yields a resistivity structure representative of the underlying geology. Correlation of the preferred 3DMT model with information from deep wells, including interpreted natural state temperature, lithology, and alteration domains, provides model validation and further confidence that useful MT data may be acquired in the vicinity of active power plants.

1. Introduction

The electromagnetic geophysical imaging technique magnetotellurics (MT) has proven to be a useful tool in both geothermal exploration and resource characterization (e.g., Peacock et al., 2020; Boseley et al., 2010). It has been recognized for many years that magnetotellurics is well-suited to resolving low-resistivity clay caps that form over high-enthalpy geothermal systems (Cumming and Mackie, 2010; Cumming 2009). Resolving the thickness and geometry of the clay cap provides important constraints on the distribution of temperature and pressure within the reservoir in the natural state, which in turn can help target wells and guide reservoir management decisions. In recent years the community has also begun to see the benefits of collecting MT data over moderate- and low-temperature geothermal systems, such as those found in the Basin and Range province of the western United States. While it may be difficult to distinguish a low resistivity clay cap from other shallow conductors in these systems, such as playa deposits and volcanic units altered to clay by meteoric weathering, they still contain good geophysical targets for deep-sensing electromagnetic techniques. Examples of such targets include the extent of an outflow plume and the depth to competent basement rock (Folsom et al., 2020; Folsom et al., 2018).

There are several obstacles to using MT data to effectively characterize operating geothermal systems. The first challenge is that the technique is vulnerable to electromagnetic noise generated by power plant infrastructure such as transmission lines and electrical substations. Production pumps, cooling fan arrays, generators and turbines can also act as near-field noise sources and pose significant problems for MT data. The second major challenge is that modeling magnetotelluric data collected in complex geologic environments, such as those that host geothermal systems (e.g., Faulds and Hinz, 2015), typically requires computationally expensive and time-consuming three-dimensional (3D) inversion. One-dimensional modeling can be useful for shallow targets and two-dimensional inversion can be helpful if specific conditions are met, but 3D MT inversion is often the most appropriate modeling approach for imaging geothermal systems. Finally, any resistivity model derived from MT data is inherently non-unique. Without relevant information from deep wells to validate interpretations it can be difficult to justify extending geologic interpretations of geophysical data into undrilled portions of the field.

The Steamboat geothermal complex in northern Nevada (Figure 1) offers an ideal environment for examining these challenges in detail and testing possible solutions for overcoming them. The Steamboat geothermal complex is an exceptionally high-noise environment. The entire complex is confined to a narrow topographic ridge that rises out of the suburbs of Reno, Nevada, a city of >250,000 people. A major highway, Interstate 580, bisects the geothermal lease block. Within the complex are six geothermal power plants, dozens of geothermal wells, pipelines, powerlines, and transmission substations that connect the power plant to the electrical grid. Resistivity models based on magnetotelluric data collected in such high-noise environments should be subject to enhanced scrutiny by developers looking to learn something about their operating fields. To be sure that geophysical anomalies of interest are not simply artifacts of noise or a poorly constrained inversion it is good practice to corroborate such features using multiple independent data sets. Following over fifty years of development history that includes the drilling of dozens of wells, operation and optimization of several power plants, and numerous geologic, geochemical, and geophysical studies, the Steamboat geothermal complex is home to a wealth of data well-suited to validating a geophysical model.

This paper presents results from a recent magnetotelluric survey collected over the Steamboat Hills geothermal complex. We show that through careful survey design, good field practices and application of modern data processing techniques it is possible to collect reasonably high-quality MT data within an operating geothermal field. We perform 3D inversion of the MT data to produce a resistivity model of the subsurface that can be used to extend down hole data into unexplored areas of the resource. We explore model validation by comparing the preferred 3D resistivity model to 1D MT inversions as well as down hole data from two deep wells, including lithology, methylene blue analysis for swelling clays, and interpreted natural state temperature profiles. We conclude with a list of recommendations for developers and contractors to consider when collecting new or in-fill MT data over other operating geothermal fields.

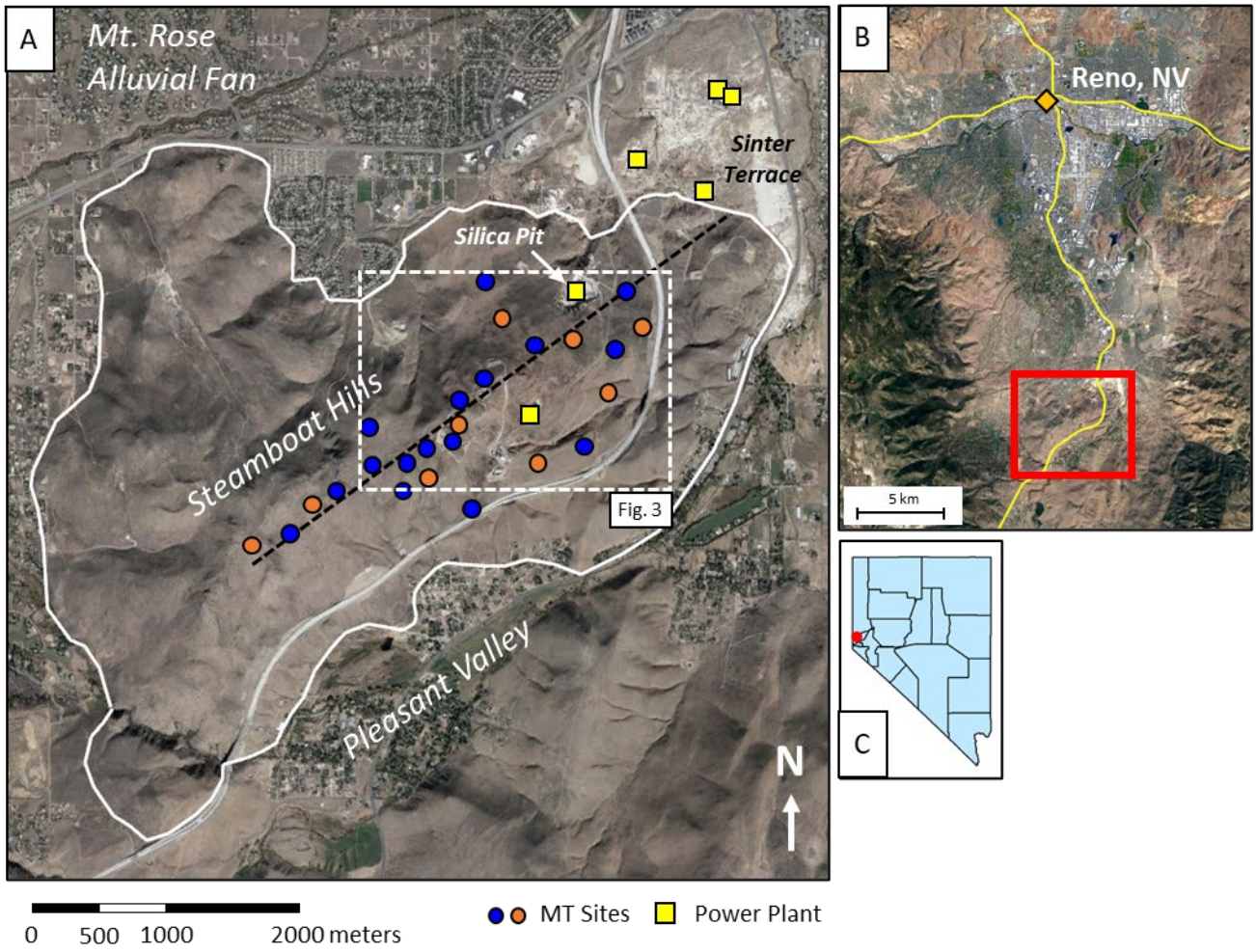

Figure 1: Location map of Steamboat geothermal complex outside of Reno, Nevada. (a) MT site locations (circles) for recent MT survey over Steamboat Hills. Blue circles are full tensor MT sites installed with magnetic field sensors; orange circles are electric-only MT sites. Black dashed line is the Steamboat Hills profile referenced in the text and shown in subsequent figures. Yellow squares are the six geothermal power plants that comprise the Steamboat geothermal complex. White solid line traces the outline of the Steamboat Hills topographic rise. White dashed line shows the extent of Figure 3. Inset maps show the location of the study area relative to (b) the city of Reno, the suburban sprawl of the Truckee Meadows, and major highways (yellow lines) and (c) the state of Nevada. Satellite imagery from Google Earth.

2. Conceptual Model Overview

The Steamboat geothermal complex is located within the Carson segment of the Walker Lane structural zone at the western margin of the Basin and Range. Right-lateral transtensional shear is accommodated by counter-clockwise rotation of fault blocks and normal displacement on a complex array of east-northeast to northwest trending structures in the northern Walker Lane (Briggs and Hammond, 2011; Cashman and Fontaine, 2000). These structures are present in the Steamboat Hills, an intra-basinal horst block in the southern Truckee Meadows composed primarily of faulted Mesozoic metasedimentary and metavolcanic rocks, intruded by Cretaceous granodiorites, and capped by Tertiary-Pleistocene volcanics (Bonham and Bell, 1993). Geophysical datasets, borehole image logs, and feed zone alignment are supportive of high-angle structures being the dominant control on permeability at Steamboat (Walsh et al., 2010; Skalbeck et al., 2002; Desormier, 1984).

Hydrothermal activity at Steamboat is likely driven by a magmatic heat source and deep circulation of large fluxes of meteoric water on high-angle structures. Fluid geochemistry and helium isotope data indicate some component of magmatic input, possibly originating from a large shallow intrusion related to the young (~1.2 Ma) rhyolitic domes near the summit of Steamboat Hills (Silberman et al., 1979). Dating of hot spring deposits and coeval volcanic units indicate that hydrothermal activity at Steamboat has persisted intermittently for >2.5 million years, with surface discharge migrating to the northeast with progressive uplift, erosion, and lowering of the water table (Silberman et al., 1979; Lynne et al., 2008). Hydrothermal fluids are relatively benign, dominated by low-TDS, Na-Cl fluids enriched in base and precious metals. CO_2/H_2S vapors mix with steam condensate in the vadose zone, resulting in extensive areas of heated ground, acid-sulfate alteration, and sulfur deposition.

The convective geothermal cell at Steamboat can be broadly described in three zones: Upper, Middle, and Lower Steamboat. Well data from Upper Steamboat suggest close proximity to ~260°C upflow, supported by close agreement between measured temperatures and silica geothermometry from reservoir fluids, coupled with broad 220-240°C temperature reversals at 800-1200 mRSL. While the local structural controls on upflow at Upper Steamboat are not well defined, permeability is likely focused along high angle structures forming a complex fault contact between granodiorite and metasediments. Three main NE-trending structures (Mud Volcano Fault, Pleasant Valley Fault, and Steamboat Fault) extend across the length of the field, linked by NW and N-S trending secondary structures. Middle Steamboat wells have encountered high-permeability zones near the intersections of the Pleasant Valley Fault and Mud Volcano Fault with NW-trending faults. These intersections are associated with thermal manifestations and zones of intense acid sulfate alteration and have been the site of high-volume injection and localized cooling. Outflow persists to the northeast towards Lower Steamboat primarily along the same main high-angle structures, although elevated background permeability in fractured host rock has also been invoked for lateral fluid flow (Johnson and Hulen, 2006). Lower Steamboat is characterized by extensive sinter and opaline silica deposits and historical surface discharge along several parallel, N-S-trending faults (Lynne et al., 2008). Lower Steamboat wells produce 140-165°C fluids at high flow rates from shallow depths (<400 m below ground level) in outflow. Tracer returns and strong pressure responses between wells provide further support for fracture linkages between Upper, Middle, and Lower Steamboat.

The Steamboat geothermal complex is wholly owned and operated by Ormat Technologies, Inc. The complex consists of six geothermal power plants with a total generating capacity of 79 MW.

3. MT Survey Design & Data Acquisition

Ormat personnel collected a total of 25 broadband MT sites at the Steamboat geothermal field over three field campaigns April 26-30, May 24-29, and November 30 – December 7, 2021. Due to limitations imposed by topography, land access, and power plant infrastructure the survey was designed as a single 3.5 km profile trending N55E, roughly parallel to the axis of the Steamboat Hills (Figure 1). Several stations were installed up to 800 m northwest and southeast of the main profile (hereafter the Steamboat Hills Profile) to increase resolution for 3D MT inversion. Station coverage includes most of Middle Steamboat, Upper Steamboat, and the crest of Steamboat Hills southwest of the geothermal lease area.

Time series data were recorded on Phoenix MTU-5C broadband receivers. Magnetic and electric field data were collected using Phoenix MTC-150 induction coils and Borin Ag-AgCl non-polarizing electrodes on 100-m dipoles, respectively. Electrodes were buried directly in shallow holes filled with locally sourced mud. Recording times varied from 18-48 hours, although most sites recorded at least 40 hours over two nights. Data were recorded on all channels at a continuous sampling rate of 150 Hz. High frequency data were also recorded at a sampling rate of 24 kHz for two seconds out of each 30 second recording interval. About one-third of the stations, mostly those located off-profile, were recorded as telluric-only sites. Full impedance tensors were determined for those sites by migrating magnetic data from nearby stations (Soyer et al., 2018). Vertical magnetic field data were collected at 15 out of 25 sites.

A dedicated remote reference MT station was installed in a rural area 50 km north of the field site and 32 km north of downtown Reno. Magnetic field data from this site, which was reoccupied for all three MT deployments, allowed for the estimation of magnetotelluric transfer functions using the robust remote reference technique of Gamble et al. (1979). Figure 2 shows magnetic field time-series data recorded simultaneously at the remote site and a site within the study area. The variation in the magnetic field observed at the remote site represents natural MT signal, in this case caused by a geomagnetic storm. The same signal is observed within the study area, demonstrating that natural MT signal can be observed above the noise in raw MT data at Steamboat.

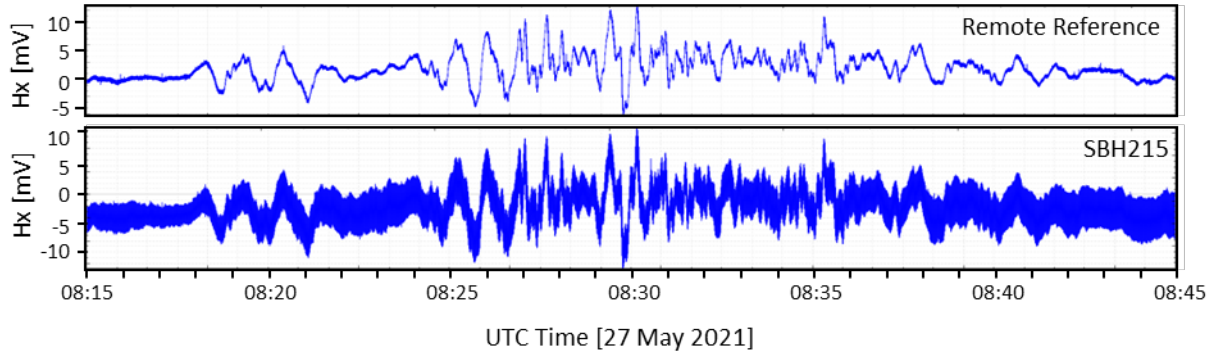

Figure 2: Raw magnetotelluric time series data recorded simultaneously at the remote reference MT site (top) and site SBH215 (bottom) during a geomagnetic storm with Kp value = 4. Plots show 30 minutes of the north-south component of the magnetic field (Hx) recorded at each site. The similarity in the two curves shows that natural MT signal can be observed above the local noise in the Steamboat MT data.

4. MT Data Analysis

Ormat personnel processed magnetotelluric time-series data to impedance tensors and vertical magnetic transfer functions using EMpower Geophysical Software (v1.54.2.5) from Phoenix Geophysics. The most effective data processing technique for improving the quality of the MT data was time masking. Windows for time masking were chosen from visual inspection of time series data (e.g., looking for spikes or offsets) and through careful trial and error to identify time windows within each day that were more likely to produce noisy data at multiple sites. These noisy time windows were then masked out of the data, leaving relatively clean estimates of MT transfer functions.

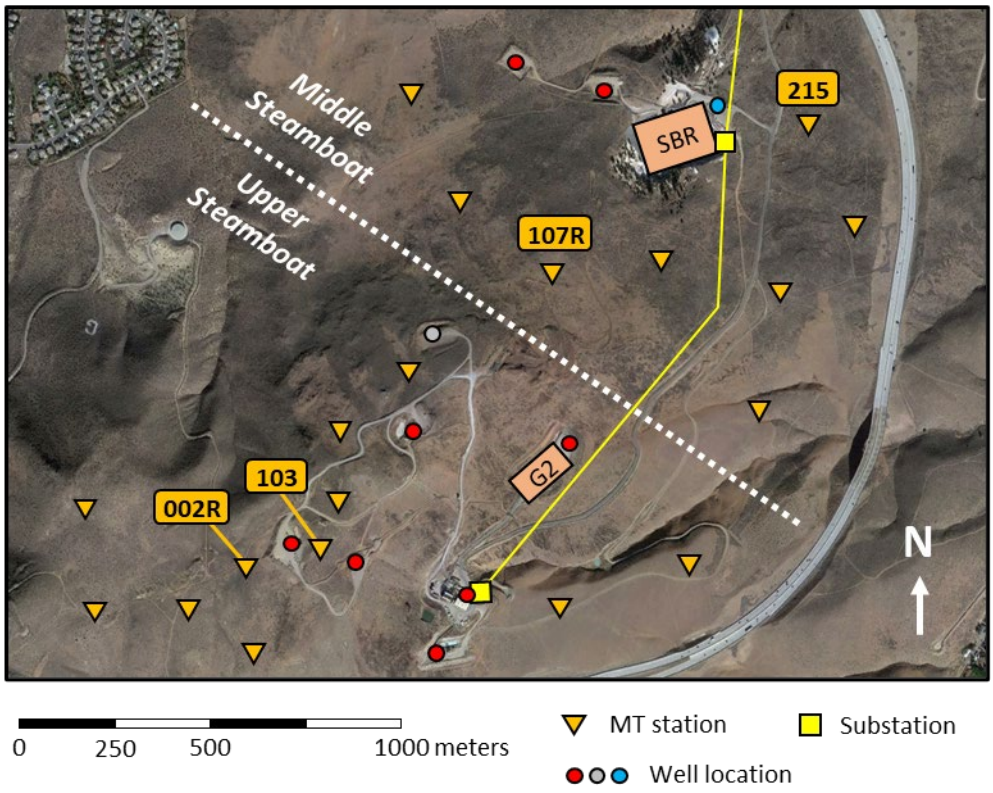

Figure 3: MT survey map showing potential noise sources in Upper and Middle Steamboat. Noise sources include power plants (tan rectangles: G2 – Galena II, SBR – Steamboat Repower), transmission lines (yellow lines), substations (yellow squares), pumped production wells (red circles), and Interstate 580 (grey line on east side of image). Power is supplied to production pumps by 60 Hz AC transmission lines draped along pipeline routes (not shown). Idle well 28-32 (grey circle) and injection well 64A-32 (blue circle) also shown. Labeled MT stations (orange triangles) correspond to plots of apparent resistivity and phase in Figure 4. White dashed line shows approximate boundary between Upper and Middle Steamboat. Satellite imagery from Google Earth.

Figure 3 shows a map of MT sites located within the Upper Steamboat geothermal complex as well as potential sources of electromagnetic noise. Other than typical 60 Hz noise, we were unable to assign any of the noise patterns we observed in time series data to any individual noise source. However, we can gain some insight by examining processed MT transfer functions in the context of where each site was recorded and what was occurring at the time of data acquisition. Figure 4 shows plots of apparent resistivity and phase for four MT sites recorded at Steamboat. For our purposes we will consider data that forms smooth curves and shows data points with small error

bars as “high quality” MT data. Figure 5 shows a run time schedule and the corresponding geomagnetic activity, represented as 3-hour averaged Kp index, for two of the sites, SBH103 and SBH215. Additional context for each of these recordings is provided below:

SBH002R – Located 150 m west of the 83-6 well pad. Production pumps on this pad were not running during the MT recording because a rig was on the pad performing a work over on one of the wells.

SBH103 – Located between two active production wells but collected while the associated power plant was shut down for maintenance in May 2021. Field crews observed various sounds coming from the infrastructure on both nearby well pads during site install, suggesting that maintenance and/or equipment testing was being performed during the shutdown. This site was almost fully encircled by pipelines.

SBH107R – Located 400 m southwest of the Steamboat Repower power plant and substation. Recorded while the plant was operating.

SBH215 – Located 250 m east of Steamboat Repower and substation but recorded while the plant was shut down for maintenance. Also located 250 m west of Interstate 580. This site may have benefited from a strong geomagnetic storm that took place during the first nine hours of data acquisition (Figures 2 & 5).

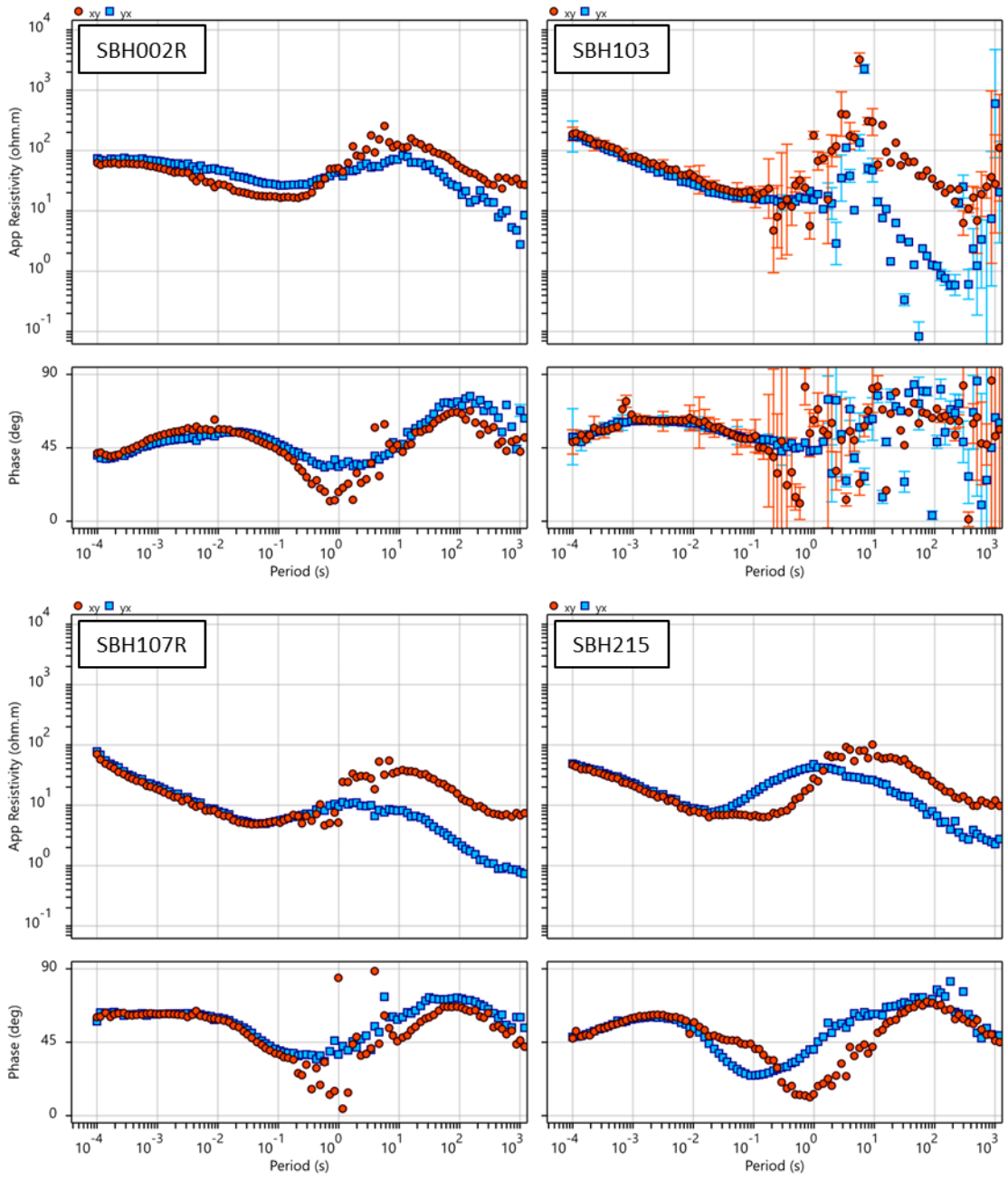

Figure 4: Apparent resistivity and phase (ρxy and ρyx) for four MT sites collected at Steamboat (see Figure 3 for site locations and nearby noise sources). Data are presented in acquisition coordinates with the x-component parallel to geographic north. All four sites recorded for >40 hours. Electrode contact resistances for all sites were <3 kΩ at install. All sites had a 60 Hz filter applied during time-series processing. See text for additional discussion.

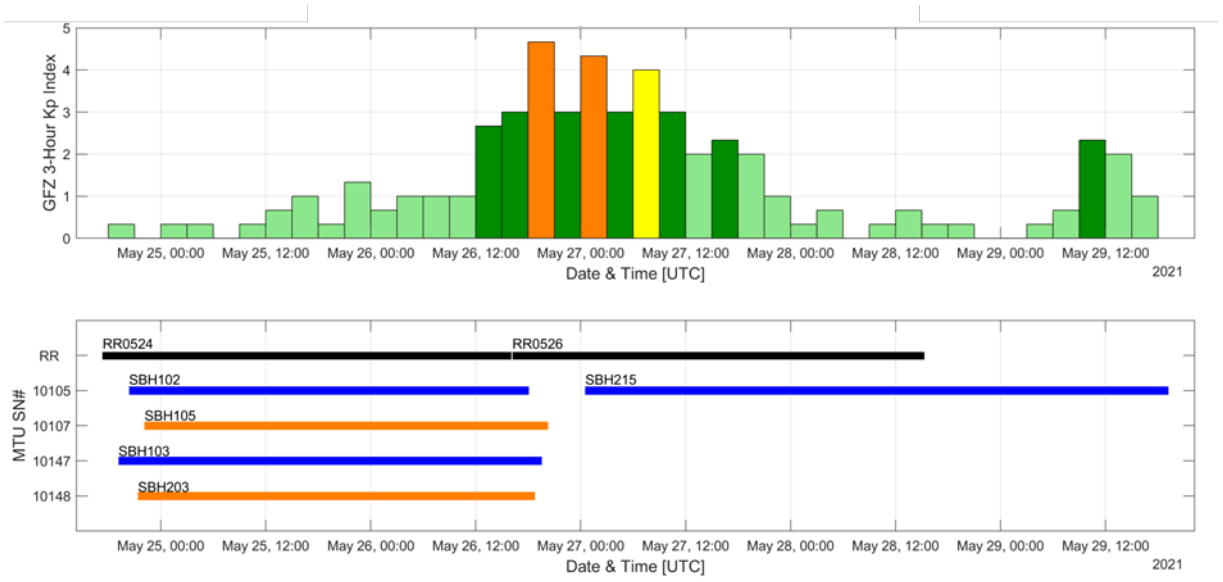

Figure 5: Example of geomagnetic storm conditions (top) and MT survey run time schedule (bottom) for May 24-29, 2021. Geomagnetic conditions shown as Kp index values averaged over 3-hour time windows (GFZ Potsdam, https://kp.gfz-potsdam.de/en/data). Kp values are a proxy for magnetotelluric signal strength and values >3 are considered favorable for MT data acquisition. Run time plots labeled by MT site name and colored by recording type: blue for five-channel full tensor recordings, orange for two-channel telluric-only recordings, and black for remote reference recordings. Note significant variability in geomagnetic signal strength over four days of data acquisition.

From these limited data we can make several observations about the influence of field conditions on MT data quality. While a plant shut down may be beneficial for some sites (SBH215 compared to SBH107R), it does not render all power plant infrastructure inert. Indeed, a plant shut down can be a valuable opportunity for the operations team to test equipment and perform maintenance, producing irregular noise sources that may be difficult to characterize or mitigate (e.g., SBH103). SBH215 demonstrates that good data can be collected within several hundred meters of a multi-lane interstate highway. It also shows the potential benefit of recording during elevated geomagnetic conditions (3-hr Kp index >3). Results from SBH002R show that decent quality MT data may be recorded in close proximity to an operating work over rig.

In general, we suspect that data quality was improved by longer recording times. It was common in the time masking workflow for individual sites or individual frequencies to benefit from multiple non-consecutive time masks that totaled more than 50% of the overall recording time. It can be assumed that with only 14 to 20-hour recordings available for some of these sites, the data would have been significantly degraded by a reduced number of "good" time windows from which to average transfer function estimates.

Of course, any adjustments to the standard practices of MT data acquisition must be balanced with logistics and survey productivity. Long recording times can be beneficial but may significantly increase the cost of the survey by adding additional field days. Multi-day recordings may also reduce the total number of stations that can be recorded if equipment and/or field time are limited. Geomagnetic activity can be reliably predicted up to three days in advance, but it can be difficult to adjust a field schedule to take advantage of good signal (or avoid days with poor signal).

5. 3D MT Inversion

To adequately represent the topography of the field site and honor the dimensionality observed in magnetotelluric phase tensor data, we decided to model the MT data using 3D MT inversion. Data and mesh preparation were carried out by Ormat personnel using the Geotools software package (v3.1.0.12474) by CGG Electromagnetics. Three-dimensional MT inversion was performed on the CGG cloud, which provides clients remote access to high performance computing resources and CGG's proprietary 3D MT inversion engine, RLM-3D (Mackie et al. 2001). Figure 6 shows a pseudo section plot of apparent resistivity data for sites along the Steamboat Hills profile (see Figure 1 for profile location). Areas where data points and contours are missing represent outliers and excessively noisy data points that were masked prior to 3D inversion.

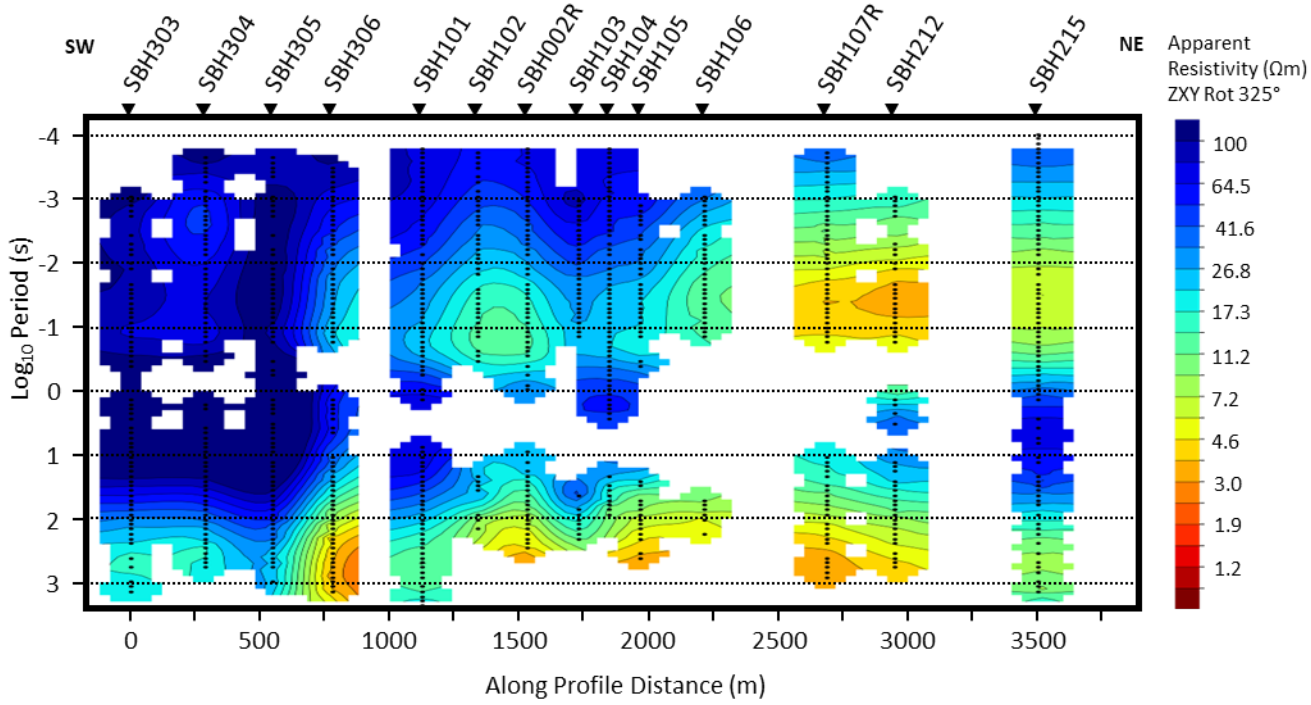

Figure 6: Pseudo section plot showing data masking for along profile MT sites used in 3D inversion. Displayed data points (black dots) were interpolated to 5 points per decade prior to 3D inversion. Background color is contoured apparent resistivity for the XY data mode, rotated to 325 degrees azimuth (E-field component oriented perpendicular to trend of the profile). Note that the 3D MT inversion included additional data from off-profile MT sites that are not displayed here.

The preferred 3D MT model was achieved by inversion in two phases. The first phase was an inversion of four-component magnetotelluric impedance data starting from a uniform half-space with resistivity 40 Ωm. That model was allowed to converge for 60 iterations and achieved a final root mean square (RMS) error of 1.63. For the second phase we added tipper data to the inversion and used the final model from phase one as the starting model. That model was allowed to converge for an additional 45 iterations and achieved a final RMS error of 1.80. Figure 7 shows RMS values as a function of frequency for the final preferred model.

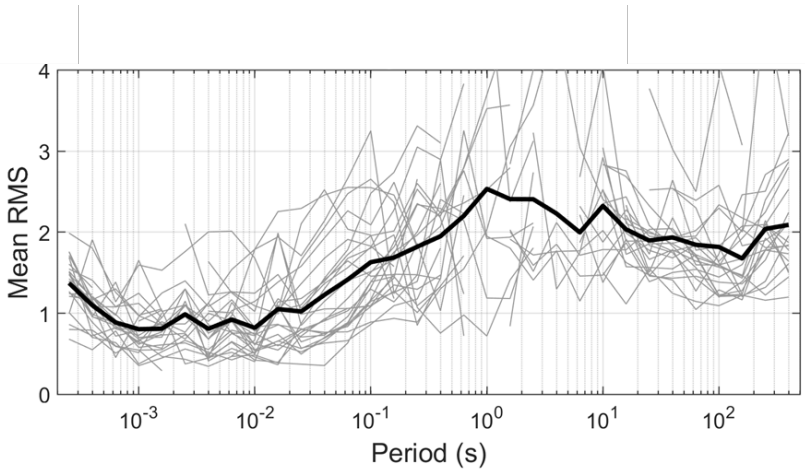

Figure 7: RMS error for the preferred 3D MT model as a function of data period. Thin gray lines are RMS plots for individual sites. Thick black line is average RMS for all sites as a function of period.

Acquisition of tipper data at select sites provided important constraints on the 3D MT inversion. Several sites with lower quality impedance data, including a few sites located within the dense infrastructure of Upper Steamboat, exhibited higher quality tipper data, suggesting that noise was more prevalent in the electric field compared to the magnetic field. The resistivity models that resulted from 3D inversions that incorporated tipper data are considered more robust because they are constrained by a higher volume of data, and they include data for sites and frequencies where impedance data may be lacking.

Figure 8 shows a cross section through the preferred 3D MT model. This model was chosen from a handful of preferred model candidates based on several criteria. The overall RMS value of the model was reasonably low and compared favorably to other models. Individual RMS values were relatively uniform for all MT sites and frequencies (Figure 7). Finally, and most importantly, this model showed the best agreement with independent data sets, including 1D MT inversions and down hole data from multiple deep wells (see next section).

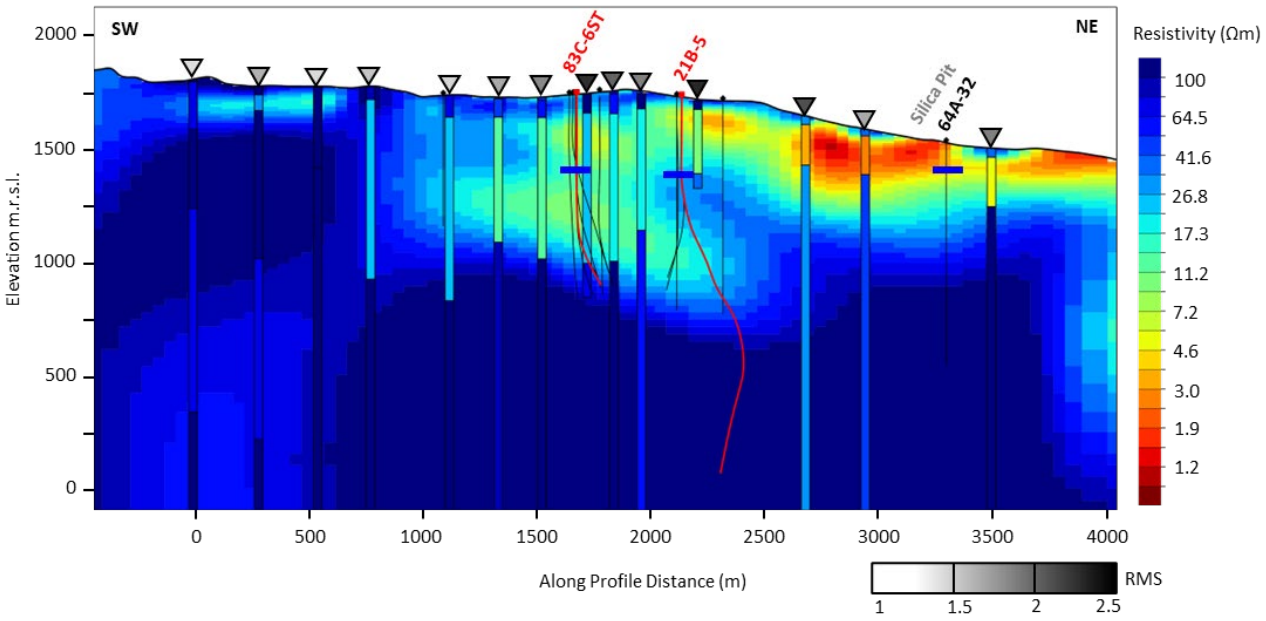

Figure 8: 3D MT model cross section for the Steamboat Hills Profile. Background color is resistivity of preferred 3D MT model. Location of MT stations along the profile indicated by inverted triangles shaded by RMS fit to 3D MT model. Vertical bars below each MT station show 1D MT inversion results (minimum structure models) for the transverse-electric mode of each MT site. Thin black and red lines are well tracks. Wells discussed in the text are labeled in black and red. Thick blue horizontal lines indicate static water levels. Surface features of interest labeled in gray.

6. Comparison of 3D MT Model to Down Hole Data

Resistivity anomalies in geothermal settings can be attributed to a variety of geologic features and subsurface conditions, including rock type, hydrothermal alteration, temperature, and groundwater fluid chemistry (Ussher et al., 2000). Down hole data from existing wells, including mud logs, alteration mineralogy, temperature, and drilling data, can provide useful constraints on the inherently non-unique interpretation of 3D MT inversion results. Data from multiple wells can refine these interpretations further and allow projection of geologic interpretations of the geophysical data into undrilled portions of the resource.

Figure 9 compares the resistivity of the preferred 3D MT model to downhole data from two deep wells drilled at Upper Steamboat, 21B-5 (total depth 5,695 ft) and 83C-6ST (TD 3,100 ft). Both wells are deviated production wells that target high-angle fault structures within the 230-240°C resource of Upper Steamboat. Data in Figure 9 are presented in elevation relative to sea level to facilitate comparison to the cross section in Figure 8.

The left column of Figure 9 shows interpreted natural state temperatures for each well alongside the results of methylene blue titration analysis on stored well cuttings. Natural state temperature profiles were interpreted by Ormat geologists by compiling and evaluating multiple pressure-temperature surveys collected under static conditions. Methylene blue (MeB) titration analysis is a semi-quantitative method for assessing the abundance of smectite clays in well cuttings (Gunderson et al., 2000). Smectite clays are typically only stable in the temperature range 70-

200°C. At higher temperatures (200-240°C) smectite transitions to mixed-layer smectite/illite and eventually pure illite, both of which exhibit less affinity for MeB dye and higher resistivity in MT models due to a reduced cation exchange capacity. The MeB titration technique has found use within the geothermal community as a rapid, inexpensive downhole geothermometer that can be deployed either while drilling or in the laboratory to map mineral alteration within a geothermal reservoir and constrain interpretations of MT resistivity models (e.g., Sepulveda et al., 2012).

The middle column of Figure 9 shows simplified lithology for each well. These geologic profiles are compiled from mud logs and geologic interpretations of the resource conceptual model. The comb-tooth pattern near the bottom of 83C-6ST (Figure 9b, below 1050 m elevation) represents a complicated zone in which multiple thin veins of granodiorite are intermixed with the older metamorphic rocks. Multiple zones of total lost circulation were observed while drilling at these depths.

The resistivity profiles shown in the right-hand column of Figure 9 were extracted along each three-dimensional well path in measured depth and then transformed into elevation. These resistivity profiles may differ slightly from those shown in Figure 8, where 3D well paths have been projected onto a 2D cross section.

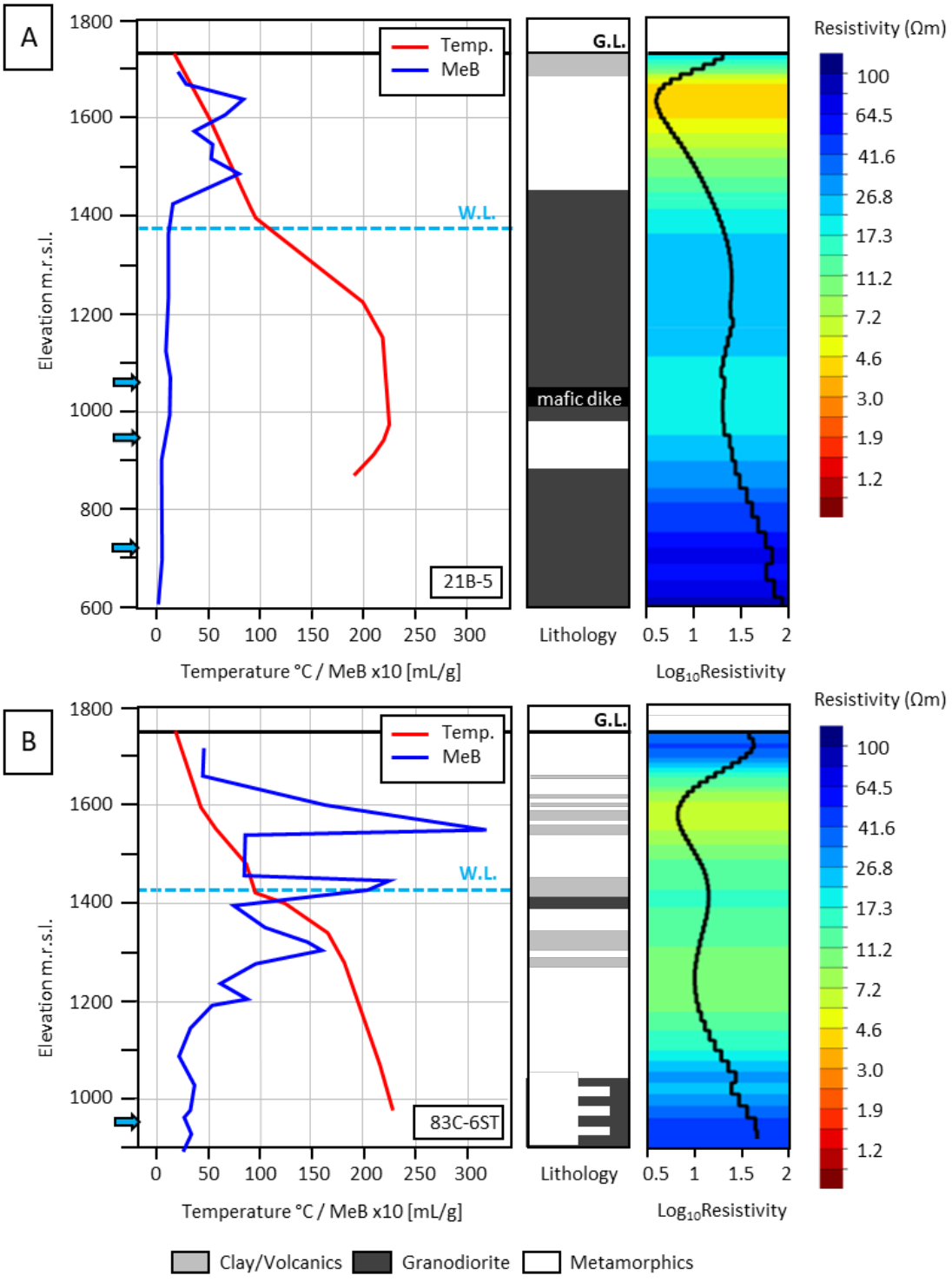

Figure 9: Down hole data for wells (a) 21B-5 and (b) 83C-6ST. Plot on the left shows methylene blue titration analysis at 100 ft intervals and interpreted natural state temperatures. Center plot shows interpreted lithology from mud logs. Plot on the right shows resistivity from the 3D MT model extracted along the well path as both a resistivity profile (black line) and resistivity pixels (background). Blue arrows represent indications of permeability encountered while drilling (e.g., no returns). W.L. = static water level. G.L. = ground level. See Figure 8 for well paths projected onto a cross section through the 3D MT model.

7. Discussion

7.1 Well 21B-5

Well 21B-5 is useful for interpreting the MT model because it is one of the few wells along the Steamboat Hills profile that crosses the high-angle contact between the Cretaceous granodiorite that comprises the basement rock in Middle Steamboat and the older metamorphic rocks encountered in most wells in Upper Steamboat. We see from comparison to the simplified lithology in Figure 9a that there is a clear correlation between the intruded granodiorite and higher resistivity values in the MT model. The lower section of granodiorite is exceptionally resistive (>50 Ωm), while the upper section is less resistive (>20 Ωm) but still distinct from the sections of metamorphic rocks above and below. This could imply that the upper section of the granodiorite has been moderately altered by the hydrothermal system, or it could simply be an artifact of model regularization that minimizes sharp contrasts in the 3D resistivity structure. We prefer the latter interpretation given that there were no indications of permeability encountered while drilling through the granodiorite in this section of the well and the MeB analysis suggests there is minimal argillic alteration in the cuttings at these depths.

The shallow low resistivity feature in well 21B-5 is likely related to hydrothermal alteration. The cross-section view through the MT model (Figure 8) and the geologic data for this well indicate this is a discrete low resistivity zone within the metamorphic rock. A weathered volcanic unit or an unaltered sub-unit of the metamorphic section that is naturally low resistivity (e.g., shale) should present as a sub-horizontal low resistivity layer in the MT model rather than a discrete anomaly. The feature exhibits a resistivity value typical of argillic alteration (<5 Ωm) and has elevated smectite content according to the MeB analysis. However, there is no hydrothermal alteration or surface manifestations observed in Steamboat Hills above the elevation of the Silica Pit (Figures 1 and 8). Drilling data suggests there is very little permeability in the shallow subsurface at Upper Steamboat and the resistivity anomaly currently resides above the water table. If this feature is a result of hydrothermal water-rock interaction, it is unlikely that those processes are occurring in the modern system at these depths. An alternate hypothesis is this feature represents relic argillic alteration from a time when the water table was higher and/or shallow permeability (since sealed) was sufficient to allow hydrothermal alteration of the country rock.

7.2 Well 83C-6ST

A key observation of the available down hole data for well 83C-6ST is the strong correlation between smectite content from MeB analysis, elevated clay content identified in the mud log, and zones of low resistivity observed in the 3D MT model (Figure 9b). There are three distinct peaks in the MeB data at 1550, 1450 and 1320 m elevation, which correspond to zones of elevated clay content according to the mud log. The shallowest peak correlates with the lowest resistivity observed along the well path (~7 Ωm) and the deepest peak corresponds to a broad zone of relatively low resistivity in the metamorphics. The middle peak is coincident with a local high in the resistivity profile, which could be an indication that this clay zone, the thinnest of the three, is below the resolution of the MT method at this depth. The relatively high resistivity may also be associated with a tongue of granodiorite that was observed in the well log near this clay zone.

We interpret the discrete zones of elevated swelling clay in this well as discrete fractures or fault damage zones associated with an older iteration of the geothermal system. Hydrothermal water-

rock interactions within permeable structures would give rise to argillic alteration. That this alteration is confined to discrete zones, and the MT model shows only moderately low resistivity values, suggests a fracture-dominated permeability regime where the country rock is largely isolated from the hydrothermal fluid and left unaltered. Given that the geothermal reservoir beneath Upper Steamboat appears to be tight above an elevation of about 950 m, it is reasonable to assume these fractures are entirely filled with clay or otherwise sealed and do not provide fluid pathways for the modern system.

Below an elevation of about 1150 m, the natural state temperature profile for this well crosses into the smectite-illite transition zone above 200°C. As temperature increases below this elevation there is a corresponding decrease in smectite content and an increase in resistivity. Clays that replace smectite at higher temperatures, such as illite and chlorite, are not detectable in MeB analyses and exhibit higher resistivity values. This suggests resistivity at this elevation is controlled by smectite content and temperature. The increase in resistivity may also be attributed to thin zones of granodiorite noted in the mud log for 83C-6ST, although we have low confidence in that particular interpretation of the lithology. There have been six wells drilled from the 83-6 well pad that all target the same structure and only a few of those well logs note granodiorite near the elevation of increasing resistivity.

We note that the "background" smectite content in this well is elevated relative to 21B-5, even if the three prominent peaks are ignored. This could be explained by pervasive, clay-filled micro fractures that are below the resolution of the well log and the MT modeling, or it may be that smectite from the clay-rich fracture zones has been smeared into deeper well cuttings through drilling.

7.3 Synthesis

Having used the available down hole data to constrain some of the major resistivity anomalies in the MT model we can expand our interpretation to some key features of the resistivity cross-section in Figure 8. Although there appears to be good correlation between low resistivity features in the MT model and argillic alteration observed in well data, it is not straightforward to map the MT model to temperature across the entire field. We do not observe a coherent "clay cap" style anomaly, i.e., there is no shallow low resistivity layer that can be used to map a particular isotherm near the upper end of the smectite stability zone (e.g., 220°C). This could be a consequence of the reservoir being comprised of two different rock types that exhibit different permeability regimes.

In well 83C-6ST, which is drilled primarily in metamorphic rocks, there is good correlation between temperature, clay content, resistivity, and permeability. Vertical permeability, especially within the smectite stability zone, seems to be low. There are no surface manifestations in Upper Steamboat and any fractures above the production zone appear to be well sealed by clay. The resistivity signature appears to be controlled by high swelling clay content in discrete fractures rather than pervasive alteration of the rock matrix. The good correlation between resistivity, temperature, and swelling clay content suggests the resistivity model might be useful in projecting temperature contours southwest of well 83C-6ST.

By contrast, the resistivity within the granodiorite basement rock appears to be controlled by permeability and less indicative of temperature. In well 21B-5, the granodiorite at intermediate depth appears to be highly resistive and unaltered despite sufficient temperatures to form swelling

clays (>70°C). This is presumably a result of exceptionally low permeability within the intrusion that prevents hydrothermal fluid from interacting with the rock. This is in contrast with the exceptionally low resistivity anomaly (<2 Ωm) observed in the same granodiorite intrusion in Middle Steamboat. The shallow subsurface in this portion of the field (2500-3500 m along profile in Figure 8) is characterized by an intense low resistivity anomaly that we interpret as acid-sulfate and argillic alteration. This interpretation is supported by connection of this feature to the Silica Pit, an area of acid-sulfate alteration exposed at the surface (Figure 8). Intense alteration beneath Middle Steamboat is likely facilitated by complex fault interactions and a high fracture density within the granodiorite that has allowed a high degree of water-rock interaction over geologic time. This permeability appears to be intact in the modern system, as evidenced by numerous lost circulation zones encountered while drilling in this portion of the field (e.g., well 64A-32, Johnson and Hulen, 2006).

Future work will focus on refining the conceptual model of the Steamboat geothermal field to fully incorporate the 3D MT results. We plan to collect additional MeB analysis for other wells in Upper and Middle Steamboat and do more work to tie the resistivity model to lithology. We expect that the MT results will be critical to understanding permeable fluid pathways and natural state temperatures in the transition zone between Upper and Middle Steamboat where there is almost no well control and few geologic structures mapped at surface.

8. Conclusions

The quality of magnetotelluric data collected near operating geothermal power plants may be improved by careful survey planning, select adjustments to standard field practices, and detailed data processing. The successful acquisition, modeling, and interpretation of broadband MT data collected at the Steamboat Hills geothermal complex provides an example of how this might be accomplished in a particularly high-noise environment. Comparison of the MT results to down hole data from deep wells is critical for model validation and allows for projecting lithology, temperature, and permeability into unexplored portions of the resource.

We offer the following recommendations for operators looking to collect and interpret high-resolution broadband magnetotelluric data in the vicinity of existing power plants:

- Install a dedicated remote reference station in a quiet location several tens of kilometers distant from the survey area. Make regular visits to the remote site to ensure it is recording for the duration of the MT survey.
- Record data for two nights (36-48 hours) to maximize the amount of data recorded during low noise time windows and/or favorable geomagnetic conditions. This is especially helpful for sites located within 1 km of active noise sources.
- Collect full tensor MT data (at least four channels) to allow for 3D inversion and/or rotation of the data into a preferred coordinate frame for 2D inversion.
- Coordinate with plant operators to schedule data acquisition during plant shutdowns.
- Methylene blue titration analysis performed on new or stored well cuttings can be instrumental in interpreting resistivity models derived from MT.

We emphasize that new or in-fill MT data may be collected at any stage in the development history of a geothermal field. The resistivity signature of a geothermal reservoir is essentially static on the multi-decade time scale of project development and operations. Peacock et al. (2022) have been

indirectly testing this assumption by collecting time-lapse 3D MT over the vapor-dominated Geysers geothermal field in northern California, USA. Although they have observed changes in the resistivity structure over time, those changes are only subtle variations in the magnitude of anomalies; the geometry of key features is largely unchanged. This implies that the resistivity signature of a geothermal reservoir, even when imaged decades into the developmental history of a field, is representative of the natural state of the system prior to utilization (or the system at its most recent maximum extent in the case of relic alteration). We suspect this is especially true for liquid-dominated reservoirs where hydrothermal alteration and stratigraphy provide the dominant signals in resistivity imaging (Ussher et al., 2000). While it is always preferrable for noise considerations to collect MT data prior to construction and operation of a power plant, there is no bad time to collect magnetotelluric data at a geothermal field.

Acknowledgement

The authors thank Ormat Technologies, Inc. for permission to publish this work. We also thank the U.S. Forest Service and Ormat operations staff for facilitating access to MT site locations on Steamboat Hills. Kristina Rossavik, Peter Drakos, and Matt Folsom contributed to the MT field work. Additional methylene blue titration analysis was performed by Adrian Wiggins. Figures 4, 6 and 8 contain images produced by the Geotools software package by CGG Electromagnetics.

REFERENCES

Bonham, H.F., Jr., and Bell, J.W. "Geologic Map. Steamboat Quadrangle." *Nevada Bureau of Mines and Geology*, Map 4Fg (1993).

Boseley, C., Cumming, W., Urzua-Monsalve, L., Powell, T., and Grant, M. "A Resource Conceptual Model for the Ngatamariki Geothermal Field Based on Recent Exploration Well Drilling and 3D MT Resistivity Imaging." *Proceedings World Geothermal Congress 2010*, Bali, Indonesia (2010).

Briggs, R.W., and Hammond, W.C. "Evaluation of Geodetic and Geologic Datasets in the Northern Walker Lane-Summary and recommendations of the Workshop" *U.S. Geological Survey*, Open File Report 2011-1282 (2011).

Cashman, P.H., and Fontaine, S.A. "Strain partitioning in the northern Walker Lane, western Nevada and northeastern California." *Tectonophysics*, 329, (2000), 111-130.

Cumming, W. "Geothermal Resource Conceptual Models Using Surface Exploration Data." Proceedings: *34th Workshop on Geothermal Reservoir Engineering*, Stanford University, Stanford, CA (2009).

Cumming, W., and Mackie, R. "Resistivity Imaging of Geothermal Resources Using 1D, 2D and 3D MT Inversion and TDEM Static Shift Correction Illustrated by a Glass Mountain Case History." *Proceedings World Geothermal Congress 2010*, Bali, Indonesia (2010).

Desormier, W.L. "Geologic Report on the Proposed Steamboat Springs Unit, Washoe County, Nevada." *Phillips Petroleum Company* (1984).

Faulds, J.E., and Hinz, N.H. “Favorable Tectonic and Structural Settings of Geothermal Systems in the Great Basin Region, Western USA: Proxies for Discovering Blind Geothermal Systems.” *Proceedings World Geothermal Congress 2015*, Melbourne, Australia (2015).

Folsom, M., Libbey, R., Feucht, D., Warren, I., and Garanzini, S. “Geophysical Observations and Integrated Conceptual Models of the San Emidio Geothermal Field, Nevada.” *Proceedings: 45th Workshop on Geothermal Reservoir Engineering*, Stanford University, Stanford, CA (2020).

Folsom, M., Lopeman, J., Perkin, D., and Sophy, M. “Imaging Shallow Outflow Alteration to Locate Productive Faults in Ormat’s Brady’s and Desert Peak Fields Using CSAMT.” *Proceedings: 43rd Workshop on Geothermal Reservoir Engineering*, Stanford University, Stanford, CA (2018).

Gamble, T.D., Goubau, W.M., and Clarke, J. “Magnetotellurics with a remote magnetic reference” *Geophysics*, 44, (1979), 53-68.

Gunderson, R., Cumming, W., Astra, D., and Harvey, C. “Analysis of Smectite Clays in Geothermal Drill Cuttings by the Methylene Blue Method: For Well Site Geothermometry and Resistivity Sounding Correlation.” *Proceedings World Geothermal Congress 2000*, Kyushu – Tohoku, Japan (2000).

Johnson, S.D., and Hulen, J.B. “A Dual Hypothesis for Thermal-Fluid Advection in the Northern Steamboat Geothermal Field, Nevada—Upflow in Ancient Breccia Pipes; Distributed Outflow in a Low-Angle Extensional Fault Zone.” *GRC Transactions*, 30, (2006), 87-96.

Lynne, B.Y., Campbell, K.A., Moore, J., and Browne, P.R.L. “Origin and evolution of the Steamboat Springs siliceous sinter deposit, Nevada, U.S.A.” *Sedimentary Geology*, 210, (2008), 111-131.

Mackie, R.L., Rodi, W., and Watts, M.D. “3-D magnetotelluric inversion for resource exploration.” *SEG International Exposition and Annual Meeting*, San Antonio, TX (2001).

Peacock, J.R., Alumbaugh, D.L., Mitchell, M.A., and Hartline, C. “Repeat magnetotelluric measurements to monitor The Geysers steam field in northern California.” *Proceedings: 47th Workshop on Geothermal Reservoir Engineering*, Stanford University, Stanford, CA (2022).

Peacock, J.R., Earney, T.E., Mangan, M.T., Schermerhorn, W.D., Glen, J.M., Walter M., and Hartline, C. “Geophysical characterization of the Northwest Geysers geothermal field, California.” *Journal of Volcanology and Geothermal Research*, 399, (2020).

Sepulveda, F., Glynn-Morris, T., and Mannington, W. “Integrated Approach to Interpretation of Magnetotelluric Study at Wairakei, New Zealand.” *Proceedings: 36th Workshop on Geothermal Reservoir Engineering*, Stanford University, Stanford, CA (2012)

Silberman, M.L., White, D.E., Keith, T.E.C., and Dockter, R.D. “Duration of Hydrothermal Activity at Steamboat Springs, Nevada, From Ages of Spatially Associated Volcanic Rocks.” *U.S. Geological Survey*, Professional Paper 458-D (1979).

Skalbeck, J.D., Karlin, R.E., Shevenell, L., and Widmer, M.C. “Geothermal Reservoir Volume Estimation from Gravity and Aeromagnetic Modeling Of the Steamboat Hills Geothermal Area, Reno, Nevada.” *Geothermal Resources Council Transactions*, 26, (2002), 443-448.

Soyer, W., Miorelli, F., Mackie, R.L. "Considering true layout geometry in magnetotelluric modeling." *24th Electromagnetic Workshop*, Helsingør, Denmark (2018).

Ussher, G., Harvey, C., Johnstone, R., and Anderson, E. "Understanding the Resistivities Observed in Geothermal Systems." *Proceedings World Geothermal Congress 2000*, Kyushu – Tohoku, Japan (2000).

Walsh, P., Martini, B.A., and Spielman, P. "High Angle Fracture-Controlled Permeability at Upper Steamboat Hills Geothermal Field, NV." *GRC Transactions*, 34, (2010), 833-837.